https://doi.org/10.5392/IJoC.2018.14.1.018

Performance Analysis of Dual-Hop MBST-ADF Relay Networks Over Quasi-Static Rayleigh Fading Channels

Min-Chan Kim
Dept. of Control and Instrumentation Engineering
Korea National University of Transportation, 50 Daehak-ro, Chungju-si, Chungbuk, 27469 Korea

Sungmook Lim
Dept. of Electronic Engineering
Korea National University of Transportation, 50 Daehak-ro, Chungju-si, Chungbuk, 27469 Korea

Kyunbyoung Ko
Dept. of IT Convergence and Dept. of Electronic Engineering
Korea National University of Transportation, 50 Daehak-ro, Chungju-si, Chungbuk, 27469 Korea

ABSTRACT

The objective of this study was to derive approximate closed-form error rates for M-ary burst symbol transmission (MBST) of dual-hop adaptive decode-and-forward (ADF) cooperative relay systems over quasi-static Rayleigh fading channels. Within a burst, there are pilot symbols and data symbols. Pilot symbols are used for channel estimation schemes and each relay node's transmission mode selection schemes. At first, our focus was on ADF relay systems' error-events at relay nodes. Each event's occurrence probability and probability density function (PDF) were then derived. With error-event based approach, we derived a tractable form of PDF for combined signal-to-noise ratio (SNR). Averaged error rates were then derived as approximate expressions for arbitrary link SNR with different modulation orders and numbers of relays. Its accuracy was verified by comparison with simulation results.

Key words*: MBST, ADF, Rayleigh Fading Channels, Average Error Rate.*

1. INTRODUCTION

Many researchers have discussed cooperative decode-and-forward (DF) relay systems, with which the DF scheme detects the received signal and then retransmits a regenerated signal [1]-[3]. With the adaptive DF (ADF) schemes, relays forward only correctly decoded messages [4], [5]. ADF schemes presume the incorporation of a cyclic redundancy check (CRC) code from a higher layer (e.g., data link layer) in order to detect errors at each relay node [3], [6]-[8]. Moreover, the author in [9] considers a forward error correction (FEC) code to decode the error at each relay node and then, shows that the CRC-based decision performs very well with message-wise block fading conditions.

At the destination node, the receiver can employ diversity combining techniques to enhance performance from the multiple signal replicas transmitted by the source and the relays. The advantages of general cooperative diversity schemes come at the expense of spectral efficiency since the source and all of the relays must transmit on orthogonal channels in order to avoid interfering with each other [3], [10].

The authors in [4] have shown a general approach applicable for both DF and ADF relaying and have derived an exact bit error rate (BER). Their work shows, only for binary phase shifting keying (BPSK), how an erroneous detection at each relay affects both the received signal-to-noise ratio (SNR) and the average BER. Note that even if their work can give exact results [4], previous researches including relay-selection schemes have assumed that each relay can detect errors symbol-by-symbol [4], [11]-[13]. That means that at each relay, the transmission or no-transmission mode can be determined symbol-by-symbol. The performance based on symbol-by-symbol implies only an achievable bound. In [14], the authors showed a practical approach covering burst transmission for ADF relay systems only for BPSK. Nevertheless, no one has expressed the error rate expressions as well-known tractable forms, which can cover M-ary PSK (MPSK) and M-ary quadrature amplitude modulation (MQAM) burst symbol transmission. Herein we extend the analytical approach in [14] and [19] to ADF burst M-ary symbol transmission systems.

* *Corresponding author, Email: kbko@ut.ac.kr*
Manuscript received Oct. 17, 2017; revised Mar. 27, 2018; accepted Mar. 27, 2018

In this paper, we consider M-ary symbol burst transmission for ADF relay systems. We focus on the analysis and evaluation of the un-coded error performance of ADF relay systems with pilot symbols. Therefore, we assume that CRC codes are used to detect burst error events at each relay node. Based on this, we focus on error-events at relay nodes for burst transmission. Then, we derive the occurrence probability for each error-event. The destination node's combined SNR is presented as one among all the possible error-events' received SNRs with each error-event's selection probability, which is derived as the occurrence probability for given error-event. Finally, we derive the probability density function (PDF) for the destination node's combined SNR over quasi-static, independent and non-identically distributed (INID) Rayleigh fading channels. Based on the derived PDF, we show that average bit error probability (ABEP), average symbol error probability (ASEP), and average burst symbol error rate (ABsER) are well-approximated by simplified expressions for arbitrary link SNRs involving channel estimation errors, modulation order, and the number of relays. Moreover, based on the derived ABsER, we obtain the achievable goodput and the averaged goodput, to investigate the effect of adaptive modulation schemes on the cell coverage extension and the spectral efficiency. We compare numerical results obtained from analytical solutions with Monte-Carlo simulations. From this, we verify that correctly decoded relay nodes can be selected from transmitted pilot symbols without additional signaling between relay nodes and the destination node. Furthermore, the performance matches well with our analytical results for all SNR regions and different modulation orders and numbers of relays.

The remainder of this paper is organized as follows: Section 2 describes the system model of dual-hop MBST-ADF cooperative relay networks. In Section 3, the derived performance expressions are presented. The numerical and simulation results are shown in Section 4 and concluding remarks are given in Section 5.

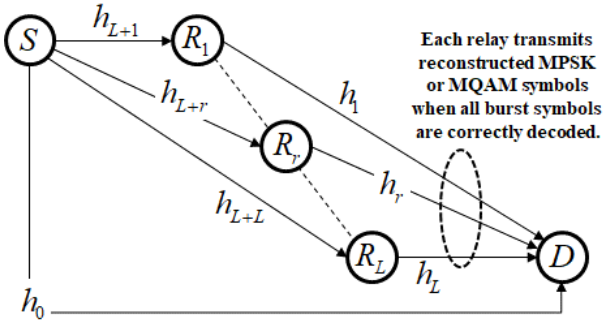

Fig. 1. Block diagram of MBST-ADF Cooperative Relay Networks (source(S), destination(D), relay(R)s)

2. NETWORK MODEL

Fig. 1 shows a block diagram of dual-hop MBST-ADF relay networks with a source (S), a destination (D), and *L* relays (R). The number of relays is *L*. In this paper, it is assumed that S and the *L* relays transmit over orthogonal time slots so that we need *L+1* time slots for single burst transmission [3]. We use a discrete time and baseband equivalent model to describe this network.

2.1 Channel and Received Signal Model

For $r \in \{1,2,\cdots,L\}$, let h_0, h_{L+r}, and h_r be the channel gains of S-D, S-R, and R-D links, respectively, as shown in Fig. 1. In this paper, wireless channels between any pair of nodes are assumed to be quasi-static Rayleigh fading [15]-[17]. That means that channel coefficients are considered to be constant during M-ary symbol burst transmissions and the magnitude and the phase of h_r are respectively Rayleigh distributed and uniformly distributed over $[0,2\pi)$. From here, N_P and N_D are the number of pilot symbols and the number of modulated data symbols within a burst. $N_B (= N_P + N_D)$ is the length of a burst. Also, each link channel is corrupted by complex additive white Gaussian noise (AWGN) term of $n_r[t]$. Without loss of generality, it is assumed that $E[|n_r[t]|]=0$, $E[|n_r[t]|^2]=\sigma^2$, and $\{n_r[t]\}$ are mutually independent for different *r* and *t*. The operator $E[\cdot]$ represents statistical expectation.

For simplicity, this paper considers the first burst transmission. Then, $s[t]|_{t=1}^{N_P} (=\pm 1)$ is the pilot symbol known to all nodes and $s[t]|_{t=N_P+1}^{N_B}$ is the M-ary phase shift keying (MPSK) or M-ary quadrature amplitude modulation (MQAM) data symbol. Also, $\{s[t]\}_{t=1}^{N_B}$ are mutually independent for different *t* with $E[s[t]]=0$ and $E[|s[t]|^2]=1$.

Within $L+1$ transmission steps, the 0th step means the source node's transmission to all the relays and the destination by using the 0th time slot. During the 0th step, the received signals can be presented, for the S-D link and the *r*th S-R link, as

$$\begin{aligned} y_0[t] &= h_0\sqrt{E_0}s[t]+n_0[t] \\ y_{L+r}[t] &= h_{L+r}\sqrt{E_{L+r}}s[t]+n_{L+r}[t] \end{aligned} \quad (1)$$

where $t \in \{1,2,\cdots,N_B\}$ and $E_0 = E_{L+r} = E_s$ is the average transmitted symbol energy of the source.

For the remaining *L* steps, each relay transmits the reconstructed data burst symbols $\{\hat{s}_r[t]\}$ only when all N_D data symbols are correctly decoded. For the *r*th time slot, the received signal at the destination node is written with $t \in \{1,2,\cdots,N_B\}$ as

$$y_0[t+rN_B] = h_r\sqrt{E_r}\hat{s}_r[t]+n_0[t+rN_B] \quad (2)$$

where E_r is the average transmitted symbol energy of the *r*th relay node. For simplicity, $y_0[t+rN_B]$ of (2) can be

expressed as

$$y_r[t] = \quad y_0[t+rN_B] = h_r\sqrt{E_r}\hat{s}_r[t] + n_r[t]$$

with $n_r[t] = n_0[t+rN_B]$.

2.2 Channel Coefficient and Noise Variance Estimation

For $1 \le t \le N_P$, $\hat{s}_r[t] = s[t]$ in (2) are pilots symbols to estimate R-D link channels so that, (1) and (2) can be expressed as single equation of $y_r[t] = h_r\sqrt{E_r}s_r[t] + n_r[t]$ with $r \in \{0,1,\cdots,2L\}$. Then, for pilot symbol based channel-estimation schemes, the channel gains can be obtained as [14]

$$\hat{h}_r = \frac{1}{N_P}\sum_{t=1}^{N_P} s^*[t]y_r[t] = h_r\sqrt{E_r} + e_r \tag{3}$$

where $e_r = 1/N_p\sum_{t=1}^{N_P} s^*[t]n_r[t]$ is the channel estimation error with $E[e_r] = 0$ and $E\left[|e_r|^2\right] = \sigma^2/N_P$. From pilot symbols and the estimated channel gain $\hat{h}_r$, the noise variance for data symbol transmission can be estimated as [14]

$$\hat{\sigma}_{D,r}^2 = \frac{N_P+1}{N_P-1}\frac{1}{N_P}\sum_{t=1}^{N_P}\left|y_r[t] - \hat{h}_r s[t]\right|^2. \tag{4}$$

The statistical noise variances for pilot and data symbol transmissions can be expressed, respectively, as

$$\begin{aligned}\sigma_{P,r}^2 &= E\left[\left|y_r[t] - \hat{h}_r s[t]\right|^2\right]_{1\le t\le N_P} = \frac{N_P-1}{N_P}\sigma^2 \\ \sigma_{D,r}^2 &= E\left[\left|y_r[t] - \hat{h}_r s[t]\right|^2\right]_{N_P<t\le N_B} = \frac{N_P+1}{N_P}\sigma^2.\end{aligned} \tag{5}$$

From (5), the noise variance ratio for pilot and data symbol transmissions can be written as

$$\frac{\hat{\sigma}_{D,r}^2}{\hat{\sigma}_{P,r}^2} = \frac{N_P+1}{N_P-1} \tag{6}$$

and it is used in (4). Note that in above equations from (3) to (6), $r = 0$, $r \in \{1,\cdots,L\}$, and $r \in \{L+1,\cdots,2L\}$ mean S-D, R-D, and S-R links, respectively.

2.3 Relay Transmission Mode Detection and MRC

For pilot-symbol transmission, we can easily assume that each relaying node can always transmits pilot symbols to the destination node. Then, the destination node can simply detect each relay's data transmission mode, and hereafter, it refers to pilot based-relaying mode selection (PB-RMS). During the *r*th time slot, we can examine pilot symbol part's power to data symbol part's power ratio (PDR) as follows:

$$\mathrm{PDR}^r = \frac{\frac{1}{N_P}\sum_{t=1}^{N_P}\left|y_0[t+rN_B]\right|^2}{\frac{1}{N_D}\sum_{t=N_P+1}^{N_B}\left|y_0[t+rN_B]\right|^2} \tag{7}$$

From (7), the *r*th relay's data transmission mode $\hat{D}_{\mathrm{Tx}}^r$ can be detected as

$$\hat{D}_{\mathrm{Tx}}^r = \begin{cases} 0, & \text{if } \mathrm{PDR}^r > 1+T_h \\ 1, & \text{else : Tx. Mode} \end{cases} \tag{8}$$

where T_h is a threshold. Note that for the given h_r, $N_P \to \infty$ and $N_D \to \infty$ lead to

$$\lim_{N_P\to\infty, N_D\to\infty}\mathrm{PDR}^r = \begin{cases} \frac{|h_r|^2 E_r}{\sigma^2} + 1 \\ 1 \qquad\quad \text{: Tx. Mode.} \end{cases}$$

Under a maximal ratio combining (MRC) at the destination node, the decision variable can be combined as

$$\hat{z}_C[t]|_{t=N_P}^{N_B} = \frac{\hat{h}_0^*}{\hat{\sigma}_{D,0}^2}y_0[t] + \sum_{r=1}^{L}\frac{\hat{h}_r^*}{\hat{\sigma}_{D,r}^2}\hat{D}_{\mathrm{Tx}}^r y_r[t]. \tag{9}$$

Note that in (9), the estimated channel gain $\hat{h}_r$ of (3) and the estimated noise variance $\hat{\sigma}_{D,r}^2$ of (4) are used.

3. APPROXIMATED ERROR PROBABILITY EXPRESSIONS

3.1 Approximated SEP for S-R Link

From $\hat{h}_{L+r}$, the *r*th S-R link's decision variable is obtained as

$$z_{L+r}[t]|_{N_P<t\le N_B} = \hat{h}_{L+r}^* y_{L+r}[t] \tag{10}$$

and then, the received SNR can be expressed as

$$\gamma_{L+r} = \frac{\left|h_{L+r}\sqrt{E_{L+r}}\right|^2}{\sigma^2(\beta_{L+r} + 1/N_P)} \tag{11}$$

with $\beta_{L+r} = E\left[|\hat{h}_{L+r}|^2\right]/E\left[\left|h_{L+r}\sqrt{E_{L+r}}\right|^2\right]$ and $E\left[|\hat{h}_{L+r}|^2\right] = E\left[\left|h_{L+r}\sqrt{E_{L+r}}\right|^2\right] + \sigma^2/N_P$. The probability density function (PDF) of random variable γ_{L+r} can be presented for the Rayleigh fading channel as

$$f_{\gamma_{L+r}}(\gamma) = \frac{1}{\overline{\gamma}_{L+r}} \exp\left(-\frac{\gamma}{\overline{\gamma}_{L+r}}\right) \text{ for } \gamma \geq 0 \quad (12)$$

with $\overline{\gamma}_{L+r} = E[\gamma_{L+r}] = E\left[\left|h_{L+r}\sqrt{E_{L+r}}\right|^2\right] / \left[\sigma^2(\beta_{L+r} + 1/N_P)\right]$.

This derivation can be applied to S-D and each R-D link by replacing $L+r$ with r, so that we can obtain γ_r, $\overline{\gamma}_r$, and $f_{\gamma_r}(\gamma)$ for $r \in \{0,1,\cdots,L\}$.

For M-ary signaling, the rth S-R link's conditional SEP can be approximated as

$$P_S(\gamma_{L+r}) \approx aQ\left(\sqrt{b\gamma_{L+r}}\right) \approx a_1 \exp\left(-b_1\gamma_{L+r}\right) \quad (13)$$

with $Q\left(\sqrt{x}\right) = 1/\sqrt{2\pi}\int_{\sqrt{x}}^{\infty}\exp(-t^2/2)dt$,

$$(a,b) = \begin{cases} (1,2) & : M = 2 \text{ (BPSK)} \\ \left(2, 2\sin^2(\pi/M)\right) & : M > 2 \text{ (MPSK)} \\ \left(4\dfrac{\sqrt{M}-1}{\sqrt{M}}, \dfrac{3}{M-1}\right) & : M > 8 \text{ (MQAM)}, \end{cases}$$

$a_1/a = 0.2$, and $b_1/b = 3.2/6$ [15-16][18-19].

3.2 Error-Event Occurrence Probability

In order to describe error-events at relay nodes, the pth error-event vector can be defined as

$$\mathbf{E}^p = \left[e_1^p \cdots e_r^p \cdots e_L^p\right] \quad (14)$$

with $p \in \left\{1,2,\cdots,2^L\right\}$ and the total number of possible error-events is 2^L. Generally, we can define that E^1 is all-zero vector, E^{2^L} is all-one vector, and so on [4][20].

For the pth error-event, $e_r^p = 0$ means that the rth relay correctly decodes N_D data symbols (i.e., $\hat{s}_r[t] = s[t]$ for $N_P < t \leq N_B$) and then, its conditional transmission mode probability can be written as

$$\begin{aligned} P_{\text{Tx}}(\gamma_{L+r}) &= \left[1 - P_S(\gamma_{L+r})\right]^{N_D} \\ &= \sum_{k=0}^{N_D}\binom{N_D}{k}(-1)^k P_S^k(\gamma_{L+r}). \end{aligned} \quad (15)$$

In addition, the average transmission mode probability can be approximated from (13) as

$$\begin{aligned} P_{\text{Tx}}(\overline{\gamma}_{L+r}) &= E\left[P_{\text{Tx}}(\gamma_{L+r})\right] \\ &= \sum_{k=0}^{N_D}\binom{N_D}{k}(-1)^k E\left[P_S^k(\gamma_{L+r})\right] \\ &\approx \sum_{k=0}^{N_D}\binom{N_D}{k}(-1)^k \frac{a_1^k}{1+b_1 k\overline{\gamma}_{L+r}} \end{aligned} \quad (16)$$

With

$$E\left[P_S^k(\gamma_{L+r})\right] \approx \int_0^{\infty} a_1^k e^{-b_1 k\gamma} f_{\gamma_{L+r}}(\gamma)d\gamma = \frac{a_1^k}{1+b_1 k\overline{\gamma}_{L+r}}. \quad (17)$$

On the other hand, $e_r^p = 1$ indicates no-transmission and its occurrence probability can be presented as $1 - P_{\text{Tx}}(\overline{\gamma}_{L+r})$. Consequently, the pth error-event occurrence probability is presented as

$$P_{\mathbf{E}^p} = \prod_{r=1}^{L}\left[P_{\text{Tx}}(\overline{\gamma}_{L+r})\right]^{\overline{e_r^p}}\left[1 - P_{\text{Tx}}(\overline{\gamma}_{L+r})\right]^{e_r^p} \quad (18)$$

with $\overline{e_r^p} = (e_r^p + 1) \bmod 2$ [4][20].

3.3 PDF of Received SNR

Under the assumption that the destination node knows correctly decoded relay nodes, the pth error-event's combined decision variable is written by using $\hat{h}_r$ and $\sigma_{D,r}^2$, from (9), as

$$z_C^p[t]\big|_{t=N_P+1}^{N_B} = \frac{\hat{h}_0^*}{\sigma_{D,0}^2} y_0[t] + \sum_{r=1}^{L}\frac{\hat{h}_r^*}{\sigma_{D,r}^2}\overline{e_r^p}\, y_r[t] \quad (19)$$

and then, its instantaneous SNR can be written as

$$\gamma_C^p = \gamma_0 + \sum_{r=1}^{L}\overline{e_r^p}\,\gamma_r = \sum_{r=0}^{L}\overline{e_r^p}\,\gamma_r \quad (20)$$

with $\overline{e_0^p} = 1$ and $\overline{e_0^p}\,\overline{\gamma}_0 = \overline{\gamma}_0$ for all p. From (12), the PDF of γ_C^p can be presented as

$$f_{\gamma_C^p}(\gamma) = \sum_{r=0}^{L}\frac{\pi_r^p}{\overline{\gamma}_r}\exp\left(-\frac{\gamma}{\overline{\gamma}_r}\right) \text{ for } \gamma \geq 0 \quad (21)$$

with $\pi_r^p = \prod_{i=0, i\neq r}^{L}\dfrac{\overline{e_r^p}\,\overline{\gamma}_r}{\overline{e_r^p}\,\overline{\gamma}_r - \overline{e_i^p}\,\overline{\gamma}_i}$ [4], [15].

Notice that when γ_C is defined as the instantaneous SNR for (9), it can be one of $\{\gamma_C^p\}_{p=1}^{2^L}$ with the probability $P_{\mathbf{E}^p}$ of (18). It means that pth PDF $f_{\gamma_C^p}(\gamma)$ of (21) can be selected as

the PDF of γ_C and then, its selection probability can be $P_{\mathbf{E}^p}$ of (18). Therefore, the PDF of γ_C can be written, for $\gamma \geq 0$, as

$$f_{\gamma_C}(\gamma) = \sum_{p=1}^{2^L} P_{\mathbf{E}^p} f_{\gamma_C^p}(\gamma) = \sum_{p=1}^{2^L} P_{\mathbf{E}^p} \sum_{r=0}^{L} \frac{\pi_r^p}{\overline{\gamma}_r} \exp\left(-\frac{\gamma}{\overline{\gamma}_r}\right). \quad (22)$$

3.4 Average Error Rate Expressions

3.4.1 ASEP for MPSK: For the given γ_C, we can express the conditional SEP as

$$P_{S,M-\mathrm{PSK}}(\gamma_C) = \frac{1}{\pi}\int_0^{(M-1)\pi/M} \exp(-s\gamma_C)\, d\theta \quad (23)$$

with $s = g_{\mathrm{PSK}} / \sin^2(\theta)$ and $g_{\mathrm{PSK}} = \sin^2(\pi/M)$ [16]. By integrating the conditional SEP of (23) with respect to random variable γ_C, ASEP can be obtained as

$$\begin{aligned} P_{S,M-\mathrm{PSK}} &= E\left[P_{S,M-\mathrm{PSK}}(\gamma_C)\right] \\ &= \sum_{p=1}^{2^L} P_{\mathbf{E}^p} \sum_{r=0}^{L} \pi_r^p \left[\frac{1}{\pi}\int_0^{(M-1)\pi/M} \overline{e_r^p}\, M_r(s)\, d\theta\right] \end{aligned} \quad (24)$$

where $M_r(s) = 1/(1+s\overline{\gamma}_r)$ is MGF of γ_r [16].

3.4.2 ABEP for MPSK: From (24), the ABEP can be approximated for MPSK as [15]

$$P_{b,M-\mathrm{PSK}} \approx \frac{1}{\log_2 M} P_{S,M-\mathrm{PSK}}. \quad (25)$$

Note that for BPSK and QPSK (i.e., M=2 or M=4), we can obtain the ABEP expression, without the approximation of (25), as

$$P_{b,M-\mathrm{PSK}}\,|_{M=1,2} = \sum_{p=1}^{2^L} P_{\mathbf{E}^p} \left[\frac{1}{2}\sum_{r=0}^{L} \pi_r^p \left(1 - \sqrt{\frac{\overline{e_r^p}\,\beta\overline{\gamma}_r/2}{1+\overline{e_r^p}\,\beta\overline{\gamma}_r/2}}\right)\right] \quad (26)$$

with $\beta = 2$ for BPSK and $\beta = 1$ for QPSK [4], [14], [16].

3.4.3 ASEP for MQAM: For the given γ_C, we can express the conditional SEP as [16]

$$\begin{aligned} P_{S,M-\mathrm{QAM}}(\gamma_C) &= \frac{4}{\pi}\left(1-\frac{1}{\sqrt{M}}\right)\int_0^{\pi/2} \exp(-s_1\gamma_C)\, d\theta \\ &\quad -\frac{4}{\pi}\left(1-\frac{1}{\sqrt{M}}\right)^2 \int_0^{\pi/4} \exp(-s_1\gamma_C)\, d\theta \end{aligned} \quad (27)$$

with $s_1 = g_{\mathrm{QAM}} / \sin^2(\theta)$ and $g_{\mathrm{QAM}} = 3/[2(M-1)]$. From (27), ASEP can be expressed as

$$\begin{aligned} P_{S,M-\mathrm{QAM}} &= E\left[P_{S,M-\mathrm{QAM}}(\gamma_C)\right] \\ &= 4\left(1-\frac{1}{\sqrt{M}}\right)\sum_{p=1}^{2^L} P_{\mathbf{E}^p} \sum_{r=0}^{L} \pi_r^p \left[\frac{1}{\pi}\int_0^{\pi/2} \overline{e_r^p}\, M_r(s_1)\, d\theta\right] \\ &\quad -4\left(1-\frac{1}{\sqrt{M}}\right)^2 \sum_{p=1}^{2^L} P_{\mathbf{E}^p} \sum_{r=0}^{L} \pi_r^p \left[\frac{1}{\pi}\int_0^{\pi/4} \overline{e_r^p}\, M_r(s_1)\, d\theta\right]. \end{aligned} \quad (28)$$

3.4.4 ABEP for MQAM: For the given γ_C and MQAM symbol, we can express the conditional BEP as

$$P_{b,M-\mathrm{QAM}}(\gamma_C) = \frac{1}{\log_2 M} \sum_{i=1}^{\sqrt{M}-1} \alpha_i \left[\frac{1}{\pi}\int_0^{\pi/2} \exp(-s_i\gamma_C) d\theta\right] \quad (29)$$

with $\alpha_i = \sum_{k=1}^{\log_2 M} \alpha_{k,i}$ and $s_i = (2i-1)^2 g_{\mathrm{QAM}} / \sin^2(\theta)$ [17] [21-22]. In [17], Tables 1, 2, and 3 show the parameters of MQAM for M=4, M =16, and M =64, respectively. From (29), ABEP can be expressed as

$$\begin{aligned} &P_{b,M-\mathrm{QAM}} \\ &= E\left[P_{b,\mathrm{M-QAM}}(\gamma_C)\right] \\ &= \sum_{p=1}^{2^L} P_{\mathbf{E}^p} \sum_{r=0}^{L} \pi_r^p \left[\frac{1}{\log_2 M} \sum_{i=1}^{\sqrt{M}-1} \alpha_i \left(\frac{1}{\pi}\int_0^{\pi/2} \overline{e_r^p}\, M_r(s_i)\, d\theta\right)\right]. \end{aligned} \quad (30)$$

3.4.5 Average Burst symbol Error Rate (ABsER) and Goodput: For the given random variable γ_C, the conditional SEP can be presented from (23) and (27) as

$$P_{S,M}(\gamma_C) = \begin{cases} P_{S,M-\mathrm{PSK}}(\gamma_C) & \text{of (23)} : \text{MPSK} \\ P_{S,M-\mathrm{QAM}}(\gamma_C) & \text{of (27)} : \text{MQAM} \end{cases}$$

and then, the conditional burst symbol error rate can be expressed as

$$\begin{aligned} P_B(\gamma_C) &= 1-\left[1-P_{S,M}(\gamma_C)\right]^{N_D} \\ &= \sum_{k=1}^{N_D} \binom{N_D}{k} (-1)^{k+1} \left[P_{S,M}(\gamma_C)\right]^k. \end{aligned} \quad (31)$$

From the approximation of (13) [15], [16], [18], $E\left[[P_{S,M}(\gamma_C)]^k\right]$ can be approximately expressed as

$$E\left[[P_{S,M}(\gamma_C)]^k\right] \approx \int_0^{\infty} a_1^k e^{-b_1 k\gamma} f_{\gamma_C^p}(\gamma)\, d\gamma = \sum_{r=0}^{L} \pi_r^p \frac{a_1^k}{1+b_1 k\overline{\gamma}_r}. \quad (32)$$

The integration of (31) with respect to the random variable γ_C gives an approximate ABsER of

$$P_B = E\left[P_B(\gamma_C)\right] = \int_0^\infty P_B(\gamma) f_{\gamma_C}(\gamma) d\gamma \approx \sum_{p=1}^{2^L} P_{\mathbf{E}^p} \left[\sum_{k=1}^{N_D} \binom{N_D}{k} (-1)^{k+1} \sum_{r=0}^{L} \pi_r^p \frac{a_1^k}{1+b_1 k \bar{\gamma}_r}\right]. \quad (33)$$

Moreover, we define the goodput form (33) as

$$\text{Goodput}_M = \log_2 M (1 - P_B) \quad (34)$$

which is the successively transmitted bits per hertz.

4. NUMERICAL AND SIMULATION RESULTS

From here on, we show numerical results for derived performance expressions and then verify their accuracy by comparing with simulation results. For simplicity, we assume $E_r = E_s / L$ for $r = 1, \cdots, L$. To capture the effect of path-loss, we define $d_r = r/(L+1)$ as the relative distance between the source and the *r*th relay. Then, the distance between the source and destination node is 1. In addition, we assume a channel model with $E\left[|h_{L+r}|^2\right] = E\left[|h_0|^2\right] / d_r^\mu$ and $E\left[|h_r|^2\right] = E\left[|h_0|^2\right] / (1-d_r)^\mu$ with the path-loss factor $\mu = 3.76$ of Table A.2.1.1.2-3 in [23] and the SNR defined as $\text{SNR} = \lim_{N_P \to \infty} \bar{\gamma}_0 = E\left[|h_0|^2\right] E_s / \sigma^2$. In addition, 'Analysis' indicates the numerical results obtained from (24), (25) or (26), (28), (30), and (33). 'Simulation' means simulation results under the assumption that the destination node can perfectly know each relay node's transmission mode. 'Simulation w/ PB-RMS' indicates the simulation results obtained from each relay transmission mode detection of (8) with $T_h = 1.0$ and (9). For the goodput performance comparison, we define the achievable goodput for adaptive modulation schemes as

$$\text{Goodput}_{\text{AM}} = \max\{\text{Goodput}_M|_{M=2,4,8,16,64}\}$$

and the average goodput for adaptive modulation is expressed as

$$\text{Average Goodput}_{\text{AM}} = \frac{1}{L+1} \text{Goodput}_{\text{AM}}$$

where the ratio of $1/(L+1)$ is caused by the fact that a *L* relaying scheme needs $(L+1)$ time slots for single burst transmission.

The plots in Fig. 2, 3, and 4 are ABEPs, ASEPs, and ABsERs, respectively. As the reference performance, error rates for the S-D link are shown in Fig. 2(a), 3(b), and 4(c). Note that the error rates for the S-D link are same for the different *L* as shown Fig. 2. As another reference performance, error rates for $N_D = 1$ are shown in all figures for *M* =2 and *M*=64. Note that for the analytical results with $N_D = 1$, the approximation of (13) is not used for the calculation of (15). In addition, we plot the results of $N_P = \infty$ which represents the case of perfect channel estimation. Note that for $N_P = \infty$, we can not use the relay transmission mode detection of (8). Therefore, 'Simulation' is presented; not 'Simulation w/ PB-RMS'.

In all figures, we can see that numerical results of 'Analysis' are well matched with simulation results for all SNR regions, modulation orders *M*, and the number of relays *L*. When we compare $N_P = \infty$ with $N_P = 8$, we can find a slight mismatch especially for lower SNRs and it is confirmed that $N_P = 8$ shows less than a 0.5dB SNR loss. Because we use the approximation of (25) for MPSK with $M > 4$, some mismatches between numerical and simulation results are shown for S-D link's ABEP with $M = 8$ in Fig. 2. For $N_P = 8$, we can see that 'Analysis', 'Simulation w/ PB-RMS', and 'Simulation' are almost the same. Note that our analysis is carried out under the perfect detection of each relay's transmission mode, as shown in (19) and (20). Therefore, this assumption is verified.

From Fig. 2, 3, and 4, we can find that average error rates increase in proportion to N_D (number of data symbols within a burst). When N_D increases, each relay's participation probability into 'Tx. mode' decreases. Consequently, it generates performance degradation shown as SNR loss in high SNR regions. Also, it is worthwhile to mention that $N_D = 1$ means the symbol-by-symbol detection of previous research [4]. The performance for $N_D = 1$ is confirmed to be an achievable lower bound for ADF relaying schemes. Even if there is performance loss according to the increase of N_D, we can still find the diversity gain caused by the increase of *L*.

Fig. 5 shows the goodput performance for the different modulation order *M* and number of relays *L*. For $L = 1$, we compare the Goodput_M of (34) according to *M* in Fig. 5(a) and it is shown that cooperative relaying schemes can be used to extend the cell coverage and the goodput gain is proportional to both *M* and the SD link's SNR. Fig. 5(b) shows Goodput_M, which is the goodput performance according to adaptive modulation schemes. The goodput enhancement can be seen as almost 10dB at SNR=10dB. As mentioned before, the goodput gain is in proportion to SNR. For $L > 1$, the goodput gain can be obtained for higher modulation and higher SNR. We can say that the cell coverage extension is achieved as the goodput gain. Note that for an *L* relaying scheme, we need $(L+1)$ time slots for single burst transmission so that there is the loss of spectral efficiency. In order to investigate this effect, we show Fig. 5(c). When we compare Fig. 5(b) and (c), it is confirmed that we can obtain the cell coverage extension without loss of spectral efficiency when the SNR is less than 18dB, 8dB, and 2dB, respectively, for $L = 1$, $L = 2$, and $L = 4$.

5. CONCLUSIONS

Approximate closed-forms are derived for averaged error rates of MBST-ADF relay systems over quasi-static INID Rayleigh fading channels. Our proposed analytical approach includes channel estimation errors related to transmitted pilot symbols within a burst. Firstly, for the relay nodes' error event, its probability is approximated using the form for the error probability of a burst MPSK or MQAM transmission. Then, the averaged error rates are derived in closed-form, to be simply calculated by numerical operations. By comparing with simulation results, the form is verified to yield an achievable error performance bounds. Furthermore, we show that the performance improvement of MBST-ADF relay systems can be considered as the goodput gain for adaptive modulation schemes. Therefore, we can conclude that our analytical expressions are in very tractable form, and can be used as a tool to verify error performance for different modulation orders and numbers of pilot and data symbols within a burst.

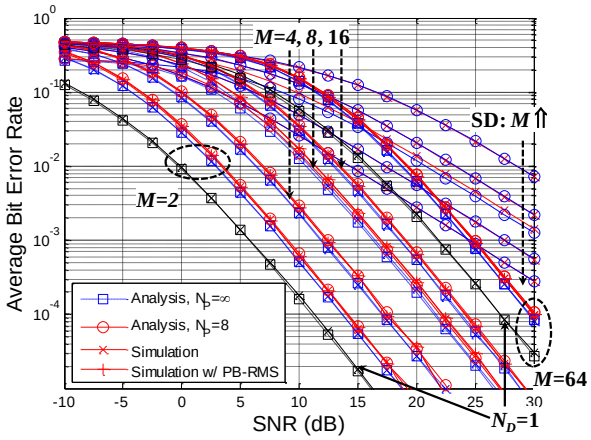

(a) L=1

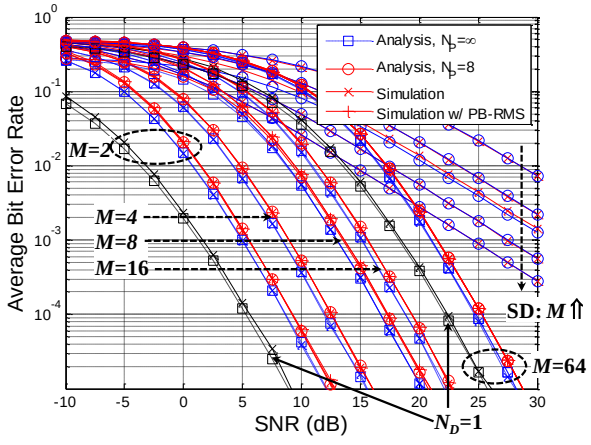

(b) L=2

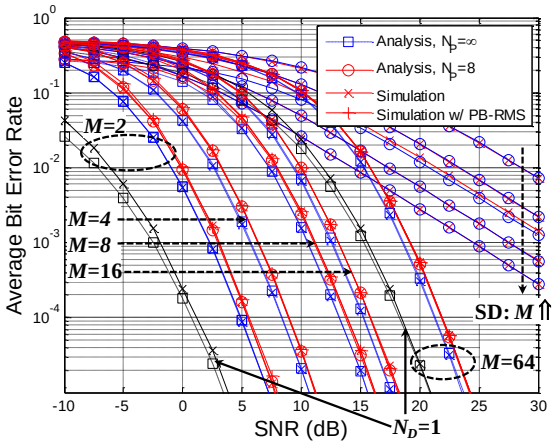

(c) L=4

Fig. 2. Average Bit Error Rate versus SNR (dB) with respect to different M and L (L=1,2,4, N_P=∞,8, N_D=1,32, M=2,4,8,16,64, μ=3.76)

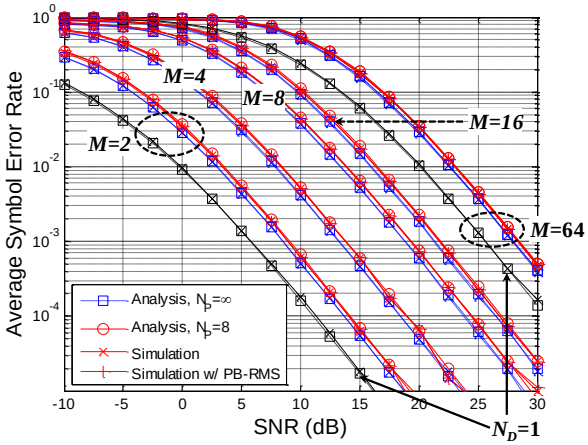

(a) L=1

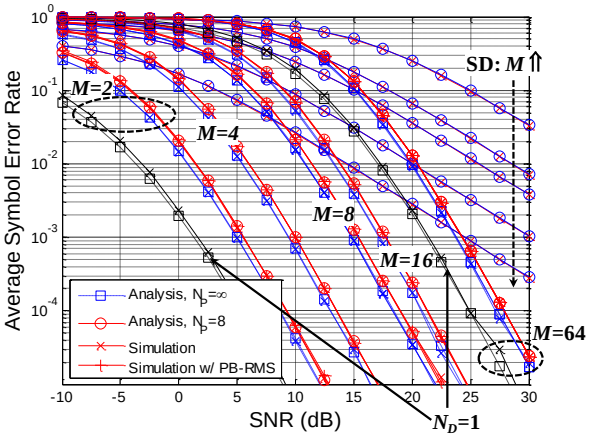

(b) L=2

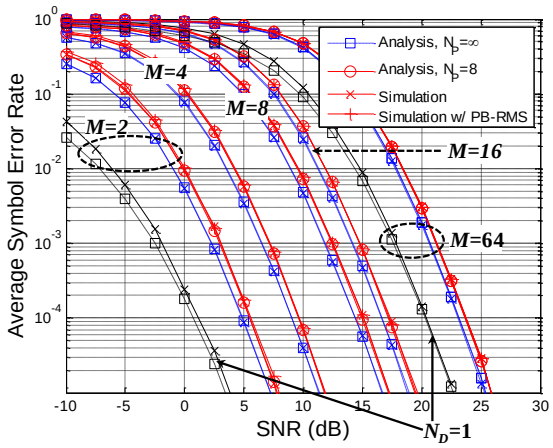

(c) L=4

Fig. 3. Average Symbol Error Rate versus SNR (dB) with respect to different M and L (L=1,2,4, N_P=∞,8, N_D=1,32, M=2,4,8,16,64, μ=3.76)

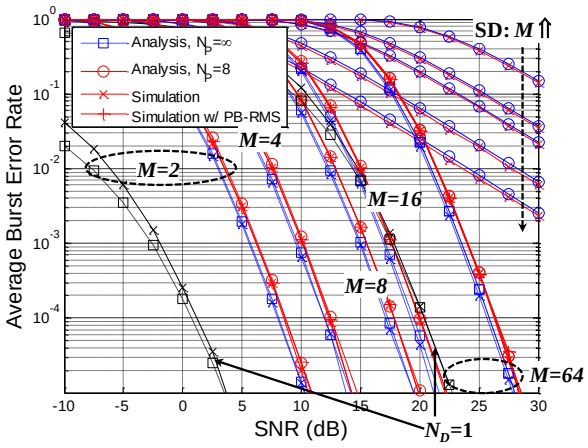

(c) L=4

Fig. 4. Average Burst Error Rate versus SNR (dB) with respect to different M and L (L=1,2,4, N_P=∞,8, N_D=1,32, M=2,4,8,16,64, μ=3.76)

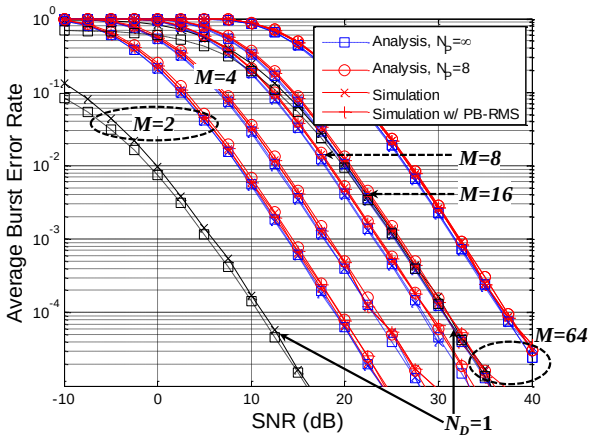

(a) L=1

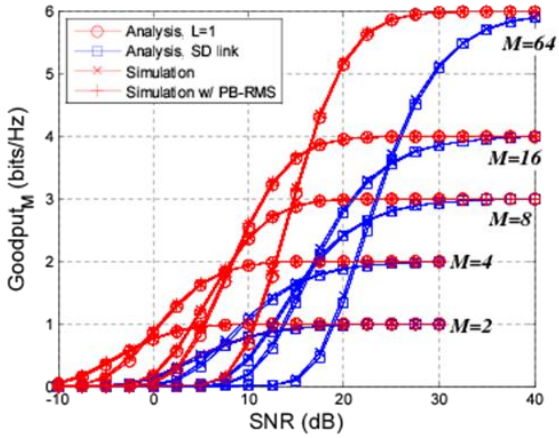

(a) $\text{Goodput}_M\,(L=1)$

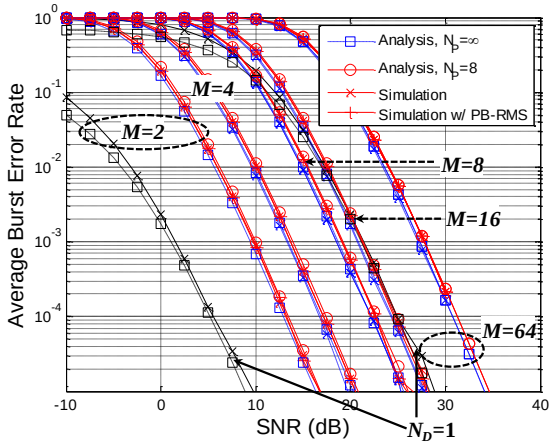

(b) L=2

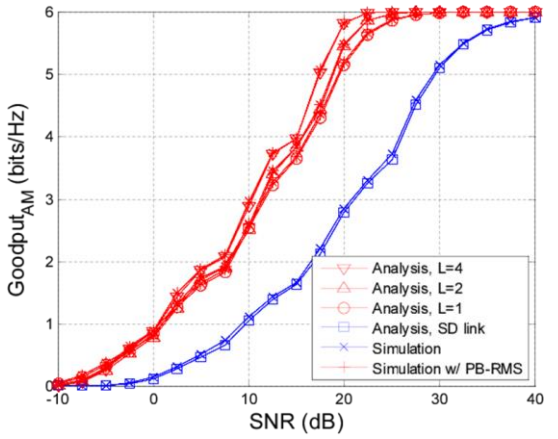

(b) $\text{Goodput}_{\text{AM}}$

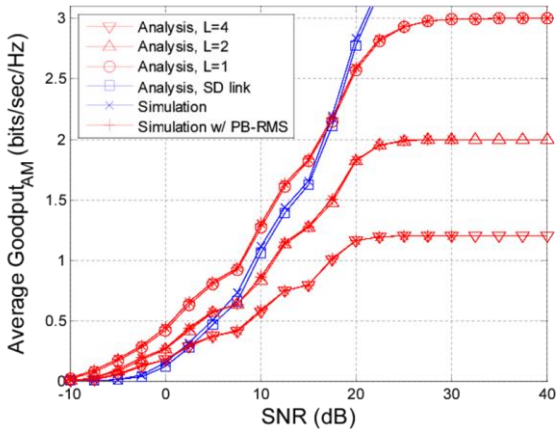

(c) Average Goodput$_{AM}$

Fig. 5. Goodput versus SNR (dB) with respect to *different L* ($L=1,2,4$, $N_P=\infty$, $N_D=32$, $M=2,4,8,16,64$, $\mu=3.76$).

ACKNOWLEDGEMENT

This research was supported by Basic Science Research Program through the National Research Foundation of Korea (NRF) funded by the Ministry of Science, ICT & Future Planning (2015R1C1A1A02037636 and 2017R1A2B4012883).

REFERENCES

[1] M. O. Hasna and M. S. Alouini, "End-to-End performance of transmission systems with relays over Rayleigh-fading channels," IEEE Trans. Wireless Commun., vol. 2, no. 6, Nov. 2003, pp. 1126-1131.

[2] P. A. Anghel and M. Kaveh, "Exact symbol error probability of a cooperative network in a Rayleigh-fading environment," IEEE Trans. Wireless Commun., vol. 3, no. 9, Sep. 2004, pp. 1416-1421.

[3] J. N. Laneman, D. N. C. Tse, and G. W. Wornell, "Cooperative diversity in wireless networks: efficient protocols and outage behavior," IEEE Trans. Inf. Theory, vol. 50, no. 12, Dec. 2004, pp. 3062-3080.

[4] J. Y. Jang and K. B. Ko, "Exact & closed-form BER expressions based on Error- Events at Relay nodes for DF Relay Systems over Rayleigh Fading channels," IEICE Trans. on Commun., vol. E94-B, no. 08, Aug. 2011, pp. 2419-2422.

[5] K. KIMURA, H. MIYAZAKI, T. OBARA, and F. ADACHI, "Signal-Carrier Cooperative DF Relay Using Adaptive Modulation," IEICE Trans. on Commun., vol. E97-B, no. 2, Sep. 2014, pp. 387-395.

[6] S. Lee, M. Han, and D. Hong, "Average SNR and ergodic capacity analysis for opportunistic DF relaying with outage over rayleigh fading channels," IEEE Trans. Wireless Commun., vol. 8, no. 6, Jun. 2009, pp. 2807-2812.

[7] S. Sagong, J. Lee, and D. Hong, "Capacity of reactive DF scheme in cognitive relay networks," IEEE Trans. Wireless Commun., vol. 10, no. 10, Oct. 2011, pp. 3133-3138.

[8] S. D. Gupta, *Forwarding Strategies and Optimal Power Allocation for Relay Networks: Forwarding Strategies and Position Dependent Optimal Power Allocation for Coherent and Non-coherent Relay Networks*, VDM Verlag, 1st ed., Apr. 2009.

[9] S. Valentin, T. Volkhausen, F. A. Onat, H. Yanikomeroglu, and H. Karl, "Enabling Partial Forwarding by Decoding-based One and Two-Stage Selective Cooperation," in Proc. IEEE ICC Workshop'08, 2008, pp. 129-133.

[10] K. B. Ko and C. W. Woo, "More Accurate ASER Bound for Opportunistic Amplify-and-Forward Relay Systems," Wireless Personal Communications, vol. 68, no. 3, Feb. 2013, pp. 609-617.

[11] S. S. Ikki and M. H. Ahmed, "Performance Analysis of Adaptive Decode-and-Forward Cooperative Diversity Networks with Best-Relay Selection," IEEE Trans. Commun., vol. 58, no. 1, Jan. 2010, pp. 68-72.

[12] K. B Ko and C. W. Woo, "Outage Probability and Channel Capacity for Nth Best Relay Selection AF Relaying over INID Rayleigh Fading Channels," International Journal of Communication Systems, vol. 25, no. 11, Nov. 2012, pp. 1496-1504.

[13] S. H. Nam, K. B. Ko, and D. S. Hong, "Exact Average SER Performance Analysis for the Nth Best Opportunistic Amplifyand-Forward Relay Systems," IEICE Trans. on Commun., vol. E95-B, no. 5, May. 2012, pp. 1852-1855.

[14] K. B. Ko and S. M. Lim, "Burst-by-Burst Adaptive DF Relay Systems with PSA-CE Methods over Quasi-Static Rayleigh Fading channels," IEICE Trans. on Commun., vol. E98-B, no. 8, Aug. 2015, pp. 1614-1621.

[15] John G. Proakis, *Digital Communication*, McGraw Hill, 3rd ed., 1995.

[16] M. K. Simon and M. S. Alouini, *Digital Communication over Fading Channels*, John Wiley & Sons, 2000.

[17] C. W. Woo, S. M. Lim, and K. B. Ko, "Performance Comparison of Dual-Hop HDAF Relay Schemes for M-QAM Burst Transmission Over Rayleigh Fading channels," International Journal of Communication Systems, vol. 30, no. 14, Sep. 2017, pp. 1-13.

[18] X. Cai and G. B. Giannakis, "Adaptive Modulation with Adaptive Pilot Symbol Assisted Estimation and Prediction of Rapidly Fading Channels," 2003 Conference on Information Sciences and Systems, The Johns Hopkins University, Mar. 12-14 2003.

[19] K. B. Ko and S. M. Lim, "Approximated Outage Probability for ADF Relay Systems with Burst MPSK and MQAM Symbol Transmission," International Journal of Contents, vol. 11, no. 1, Mar. 2015, pp. 7-14.

[20] K. B. Ko and C. W. Woo, "More Tractable Average Error Rate Expression for the Nth Best Relay Selection scheme of DF Relaying over Rayleigh fading Channels," International Journal of Communication Systems, vol. 25, no. 10, Oct.2013, pp. 1356-1364.

[21] D. J. Kim, K. B. Ko, J. H. Park, and D. S. Hong, "Average BER Analysis for Multicode 64-QAM CDMA Systems

with an MPIC," IEICE Trans. on Commun., vol. E92-B, no. 02, Feb. 2009, pp. 636-639.
[22] K. B. Ko, D. S. Kwon, D. S. Cho, C. E. Kang, and D. S. Hong, "Performance analysis of a multistage MPIC in 16-QAM CDMA systems over multipath rayleigh fading channels," in Proc. IEEE VTC 2003-Spring, vol. 4, 2003, pp. 2807-2811.
[23] 3GPP TR 36.814 V9.0.0, *Evolved Universal Terrestrial Radio Access (E-UTRA); further advancements for E-UTRA physical layer aspects*.

Min-Chan Kim
He received the M.S. degrees in the Department of Control and Instrumentation Engineering at Korea National University of Transportation, Chungju, Korea in 2012. Currently, he is working toward the Ph.D. degree in the Department of Control and Instrumentation Engineering at Korea National University of Transportation. His current research interests include the field of wireless communications focusing on cooperative relaying, ITS, and Industrial Filed Bus Communications.

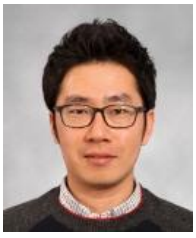

Sungmook Lim
He (corresponding author) received the B.S. and Ph.D. degrees in Electrical and Electronic Engineering at Yonsei University, Seoul, Korea in 2005 and 2012, respectively. From September 2012 to March 2014, he was a Postdoctoral Fellow at Yonsei University where his research interests were in 5G wireless communications. Since March 2014, he joined the Department of Electronics Engineering at Korea National University of Transportation as an Assistant Professor. His current research interests include the field of 5G wireless communications focusing on multicarrier and multi-antenna systems, cooperative relaying, and ITS.

Kyunbyoung Ko
He received the B.S., M.S., and Ph.D. degrees in Electrical and Electronic Engineering at Yonsei University, Seoul, Korea in 1997, 1999, and 2004, respectively. From March 2004 to February 2007, he was a senior engineer in Samsung Electronics, Suwon, Korea where he developed Mobile WiMAX systems for broadband wireless services. Since March 2007, he joined the Department of IT Convergence and Department of Electronics Engineering at Korea National University of Transportation as an Associate Professor. His current research interests include the field of wireless communications focusing on multicarrier and multi-antenna systems, cooperative relaying, and ITS.